Int J. Multiphase Flow Vol. 8, No. 1, pp. 71–82, 1982
Printed in Great Britain.

0301-9322/82/010071-12$03.00/0
Pergamon/Elsevier

FLUID-DYNAMIC INTERACTION BETWEEN TWO SPHERES

YUTAKA TSUJI, YOSHINOBU MORIKAWA and KOZO TERASHIMA
Osaka University, Suita, Osaka, Japan

(*Received* 4 *February* 1981; *in revised form* 22 *May* 1981)

Abstract—Experiment of fluid-dynamic interaction between two spheres was conducted to obtain basic information concerning the two-phase flow, especially in dense phase. Two or three spheres were set up in a water tunnel in the longitudinal or transverse direction with Reynolds numbers less than 10^3. The flow behind the sphere was visualized by the use of condense milk and change in vortex structure due to the interaction was observed in detail. Additionally, drag force on the sphere was measured by a pendulum method which was developed to detect small drag, and the range of distance in which the drag is affected by the interaction was shown.

1. INTRODUCTION

As the importance of two-phase flow increases in various kinds of industries, more investigations are required for the flow around the sphere. Generally, the two-phase flow can be regarded as a set of flow around the sphere or particle. Mutual interaction between the particles and fluid determines the macroscopic properties of the flow. Among various two-phase flows, the case of very fine particles permits sophisticated theoretical treatments to some extent, because the Stokes law is applicable. Therefore, such two-phase flows have been studied by many theoretical workers. On the other hand, two-phase flows of large particles are usually studied experimentally, because the particles are so large that the flow condition is far beyond the Stokes region. The present work was made with a mind to the case of large particles.

In order to fundamentally understand the two-phase flow, the effects of various factors on the flow around the sphere must be known. In fact there are a number of reports available about such effects as free-stream turbulence (Torobin & Gauvin 1960), velocity shear (Bagnold 1974), particle rotation (Bagnold 1974) and unsteadiness (Torobin & Gauvin 1959, Marchildon & Gauvin 1979, Karanfilian & Kotas 1978). However some problems have not yet been investigated satisfactorily inspite of the importance. Fluid dynamic interaction between spheres is one of those examples. Particularly quantitative studies of the subject are very scarce. This research situation is in contrast with the case of circular cylinders, of which interaction has been studied by many workers.

When the particle concentration is not high, fluid dynamic force on a suspended particle can be assumed to be the same as that on a single particle without the interaction. However at a high concentration rate, the effect of mutual interaction between the particles should be taken into consideration. Recently, Lee (1979) measured the drag force on the sphere under the influence of interaction at Reynolds numbers of about 10^4 (the Reynolds number is defined by the diameter of the sphere and the relative velocity). Considering that Reynolds numbers are at most 10^3 in ordinary two-phase flows, an experiment at Reynolds numbers less than 10^3 is desired to apply the results to real two-phase flows. Unfortunately, the less the Reynolds number, the more difficult the detection of the force. The present authors attempted a measurement at Reynolds numbers less than 10^3 but the lower limit of the number is about 100 due to the limit of accuracy of the measurement. As an interesting matter, the vortex behind a sphere has a coherent structure in the above range of Reynolds number. Hence, the effect of interaction on the coherency was investigated by visualizing the vortices as well as the drag measurement. With respect to the set-up of spheres, there were two cases in this experiment, i.e. two spheres in the longitudinal direction and three spheres in the transverse direction against the uniform stream.

2. EXPERIMENTAL ARRANGEMENT

An open type water tunnel of 300 × 300 mm in cross section and 5 m in length was used. A part of the side wall was made of transparent glass through which the flow could be observed. The free stream turbulence intensity measured by a hot wire anemometer was about 2.5%.

2.1 *Method of flow visualization*

Figure 1 shows the set-up of the spheres in the flow visualization. The diameter of the sphere ranged from 18 to 30 mm. The sphere was supported by a pipe of small diameter. The spheres arranged in the transverse direction were connected with each other by a rod of 1 mm in diameter. Commercial condense milk was used to visualize the flow. The milk was driven to the injection outlet through the supporter made of the pipe. The supporter had a double structure near the sphere, as shown in figure 2. The milk was first injected from the holes in the inside pipe, flowing along the annulus, and finally reached the stagnation point. This injection method enabled the milk to uniformly wrap the sphere and show the three dimensional structure of wake clearly. In the case of the rear sphere which was supported in a different way from that of the front sphere, the milk was injected from inside the sphere at the stagnation point. In the set-up of three spheres in the transverse direction, the milk injection was made only from the center sphere. When the separation position was measured, the flow was visualized not by injecting the milk but by coating the sphere with milk following Taneda (1956). Another point in the present technique is that the specific weight of milk must be coincident enough with that of water, because the free stream velocity was very low like several centimeters per second. Therefore, the specific weight was adjusted to unity by adding ethyl alcohol to the milk. In case of difficulty to distinguish the wakes from both front and rear spheres, the milk from one of the sphere was colored by red dye, rhodamine. The results of flow visualization were recorded using a 34 mm camera and 8 mm cine camera.

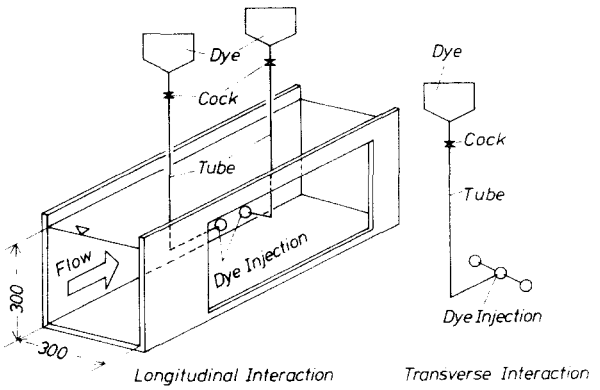

Figure 1. Experimental set-up.

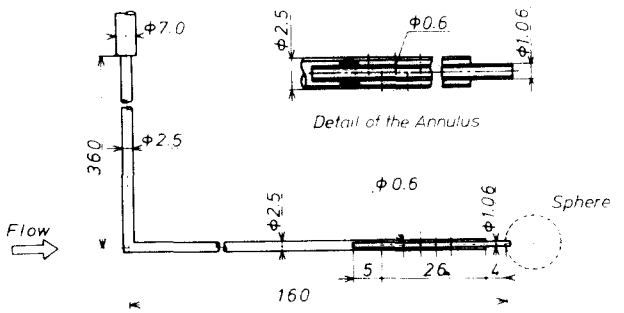

Figure 2. Details of support.

2.2 *Measurement of drag force*

The fluid dynamic force on a sphere is, generally speaking, large enough when the Reynolds number is high, so that the force on the sphere can be measured by detecting the force acting on a supporter. In the case of small Reynolds number, the drag is small but it also can be obtained from the velocity of a sphere falling freely in a fluid at rest. However, the method using such falling velocity is not suitable to the present purpose, because it is difficult to keep the distance between the spheres constant during the time of falling. To cope with these problem, "a pendulum method" was attempted in this work. In 1926, Knodel (1926) used this method to measure the drag of a sphere in pipe flow. So far as we know, it seems that this method has been scarcely used since his work. The pendulum method is convenient for the drag measurement at intermediate Reynolds numbers and so a brief description of the method which the authors adopted is given below.

Figure 3 shows principle of the method, in which a sphere with the specific weight slightly higher than unity is hung by a thin string. The drag force is measured by the amount of displacement of the sphere from the position of the stationary state, as the drag is balanced with the tension of the string and the gravity. The relationship of this force balance can be deduced geometrically from when we call a force diagram. Strictly speaking, the drag force on the string distributes along it, and thus the center of force on the string differs from the center of sphere. However when the total length L of the string is large enough compared with the length l of string dipped in the water, the force D can be assumed to act on the center of sphere like the force F. The above approximation gives

$$F + D = g(W - \rho V)X/(L - Y) \qquad [1]$$

where g is the gravitational constant, ρ, the density of water, W, the mass of sphere, V, the volume of sphere, and X and Y are the amounts of displacement of the sphere in the directions parallel and normal to the flow, respectively. Drag coefficients, C_D and C'_D are defined for F and D, respectively,

$$F = C_D q \frac{\pi}{4} D_{sp}^2 \qquad [2]$$

$$D = C'_D q d(1 - Y) \qquad [3]$$

where q is the dynamic pressure of the uniform stream, and D_{sp} and d are the diameters of the sphere and string (circular cylinder). Substituting [2] and [3] into [1],

$$C_D = [(W - \rho V)X/(L - Y) - C'_D q d(1 - Y)]/\left(q \frac{\pi}{4} D_{sp}^2\right) \qquad [4]$$

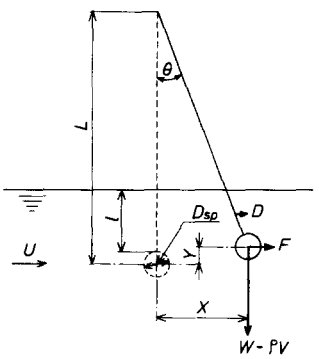

Figure 3. Principle of drag measurement.

C_D' is given as a function of the Reynolds number Ud/ν. Hence C_D is obtained by measuring X and Y, because all other quantities are known. The method described above can be easily extended to the case of flow interaction, if a dummy sphere is set up in front or rear the test sphere. Figure 4 shows such an arrangement where the effect of longitudinal interaction is investigated. It is also possible to apply this method to the case of transverse interaction, if a group of spheres connected by a rod in the transverse direction is hung by two strings. In the present experiment, a group of three spheres was supported by the two strings attached to the side spheres, and the displacement was measured in the same way as the case of a single sphere. However, we needed an assumption to deduce the drag of each sphere in the transverse interaction. That is, the drag was assumed to be the sum of f_0, the drag without the interaction and Δf corresponding to the effect of the interaction on one side. Therefore, for the side sphere, the drag is expressed,

$$f_s = f_0 + \Delta f \qquad [5]$$

and for the center one,

$$f_c = f_0 + 2\Delta f \qquad [6]$$

because the center sphere is influenced by the interaction on its both sides. Therefore, the total drag F of the three spheres including the rod is given as

$$F = 3f_0 + 4\Delta f + R \qquad [7]$$

where R represents the drag on the rod which is estimated in the same way as that of the string. The authors adopted [5]–[7] as approximations for obtaining the effect of transverse interaction on the drag. Results of the accuracy are shown later. Other details of the drag measurement are as follows. The string we used was a fishline of 1 mm in length and 0.1 mm in diameter. The spheres had the same size as those used in the visualization experiment. The motion of the sphere was tracked by a telescope and the displacement was recorded at intervals of 5 seconds, because the sphere was not rigidly supported and thus fluctuated more or less.

3. RESULTS OF FLOW VISUALIZATION

Generally, reports of the flow observation around the sphere are much fewer than those of circular cylinders. As for the vortex behind the sphere, there are papers by Taneda (1956, 1978), Magarvey & Bishop (1961), Magarvey & Machatchy (1965), Achenbach (1974) and Perry & Lim (1978). Perry & Lim (1978) controlled shedding of vortices and succeeded in observing the

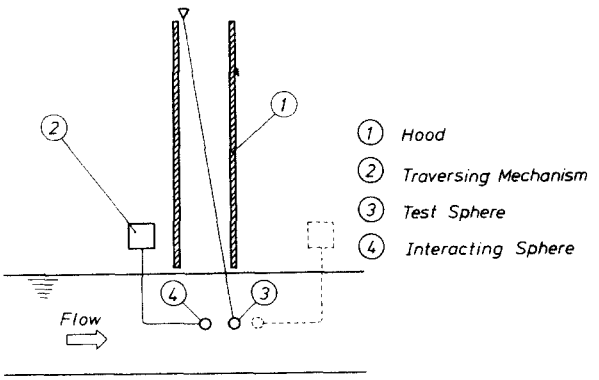

Figure 4. Set-up of spheres in the longitudinal interaction.

structure in detail. Vortices in the present experiment were natural ones, and in the case of a single sphere, we could not get more than the results by earlier workers. Thus the previous results are refered to as a standard to examine the accuracy of the present experiment, because the present flow suffered various disturbances such as the big supporter for injecting milk and comparatively high free stream turbulence. First, the results of the single sphere will be shown.

Figure 5 shows photographic pictures of vortices from the single sphere. Figure 5(a) represents the case of a low Reynolds number, where an axisymmetrical vortex attaches on the sphere. This vortex corresponds to the twin vortex on the circular cylinder, but the vortex on the sphere keeps attaching on the surface up to the Reynolds number Re = 400 from which the sphere starts to shed the vortex. Figure 5(b) shows such shedding vortices. The shedding frequency f was measured by counting the number of visualized vortices during a certain period.

Figure 6 shows the angle of the separation position, in which the present results are compared with the result by Taneda (1956). The present results are found to be on an extension of Taneda's curve. The relation between the Strouhal number $\mathrm{St} = fd/U$ and the Reynolds number $\mathrm{Re} = UD_{sp}/\nu$ is shown in figure 7 which indicates that the present results agree with the results by Möller (1938). Good agreement with the results by Taneda (1956) was obtained also with respect to the size and center of the attached vortex beside the separation angle and shedding frequency. Hence we could confirm that the present flow was a standard one.

3.1 *Longitudinal interaction*

Figure 8 shows sketches of the vortex pattern with the longitudinal interaction at a relatively low Reynolds number, Re = 220. The sketches include cases of three non-dimensional distances I_X/D_{sp}, where I_X is the longitudinal distance between sphere centers. Figure 8(a) is the case of $I_X/D_{sp} = 1$, i.e. two spheres are attached with each other. A vortex ring is confined between the spheres and the vortex from the rear sphere is almost the same as that from a single sphere.

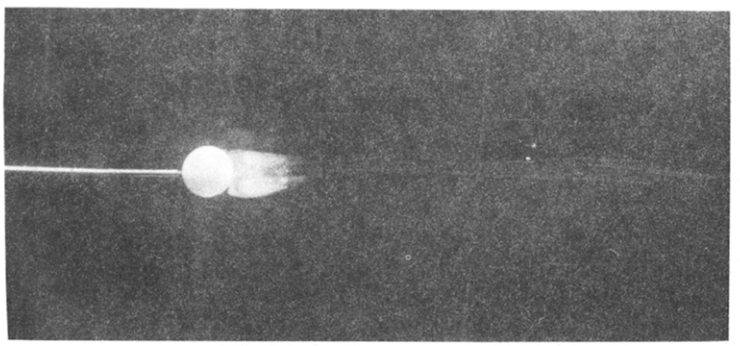

(a)

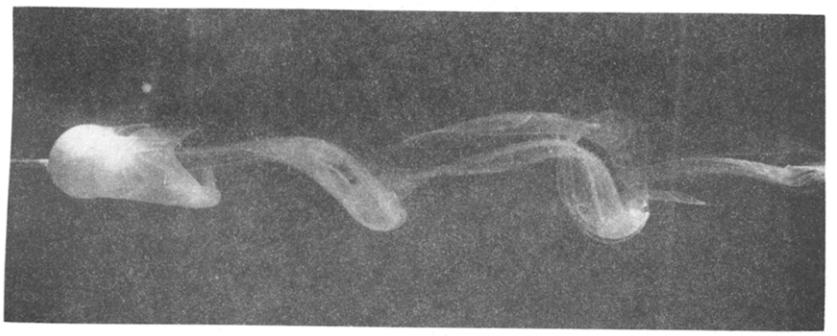

(b)

Figure 5. Vortices behind a single sphere. (a) Re = 230, (b) Re = 430.

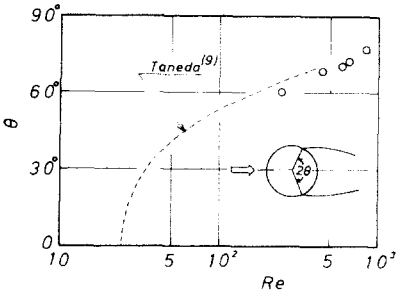

Figure 6. Separation angle vs Reynolds number.

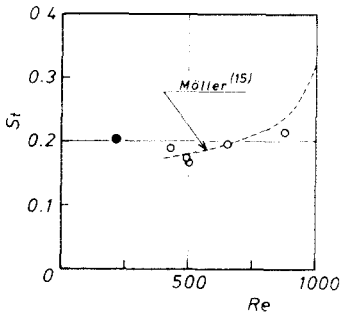

Figure 7. Strouhal number vs Reynolds number; O, single sphere; ●, front sphere with longitudinal interaction.

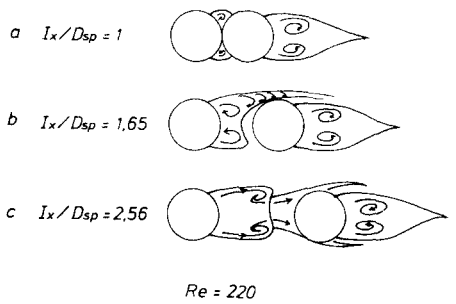

Figure 8. Schematic representation of the vortex configuration in the longitudinal interaction at Re = 220.

When the two spheres are apart at a small distance, the vortices show the pattern in figure 8(b), which is the case of $I_x/D_{sp} = 1.65$. The front vortex can not keep being confined and is carried away downstream, forming un-axisymmetrical vortex sheet. The motion of this vortex sheet is continuous and thus does not show intermittent shedding. The present vortex sheet is similar to what Taneda (1978) observed at very high Reynolds numbers in a single sphere. In contrast to the front vortex, the rear vortex is not different from the vortex without interaction. As the distance increases, the vortex shows the pattern given in figure 8(c). The front sphere sheds the vortices regularly even though the Reynolds number is not high. St number of this shedding vortex was found to be about 0.2 which is approximately the same value as is found at the Reynolds number more than 400. For comparison, that St number is plotted in figure 7. When the distance increases further, the above vortex shedding ceases and the pattern becomes the same as found behind a single sphere without interaction.

Figure 9 shows the case with two spheres attaching at Re = 440. The front sphere sheds the vortices regularly like the rear sphere, while a confined vortex ring is formed between two spheres at a small Reynolds number as described earlier in this paper. The vortex shedding is consistently observe with increasing distance between two spheres, although the vortices from both spheres are interwined and the pattern becomes complex. Moreover, both front and rear

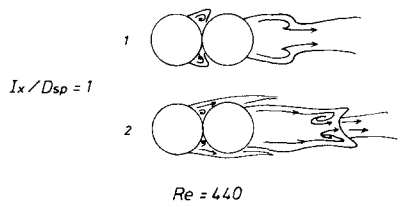

Figure 9. Schematic representation of the vortex configuration in the longitudinal interaction at Re = 440.

spheres shed the vortices at the same frequency as the single sphere. Therefore, there is no difference in St number between the cases with and withoug interaction as shown in figure 10. The above results of St number are contrasted with the results of cylinders. According to Ishigai *et al.* (1971) and Okajima (1978) who investigated the flow interaction between two cylinders, St number increases with decreasing distance between the cylinders, when the distance is less than $I_X/D = 3.8$, where D is the diameter of the cylinder.

We found above that the front vortex is much more affected by the interaction than the rear vortex. Regarding the separation position on the sphere, the results are reversed, i.e. the separation angle on the front sphere is not changed while the angle on the rear sphere decreases, as shown in figure 11.

3.2 *Transverse interaction*

Transverse interaction of cylinders has been investigated by several workers who indicated that the effect of interaction appears within I_Z/D less than 2 (Bearman & Wadcock, 1973). In the case of spheres, the vortex pattern becomes very complex under the interaction influence, because the vortex behind the sphere is three dimensional. Thus we observed the vortices only from the center sphere among the three. Vortex patterns are shown in figure 12, where four cases are presented, i.e. a large distance between the spheres ($I_Z/D_{sp} = 4.8$), moderate distance ($I_Z/D_{sp} = 2.20$, 1.48) and the case that the three spheres attach with each other ($I_Z/D_{sp} = 1$). When the distance I_Z/D_{sp} is 4.8 and 2.20, the vortex patterns are the same as in the case of the single sphere. However, the pattern of $I_Z/D_{sp} = 1.48$ shows a structure similar to the Kármán

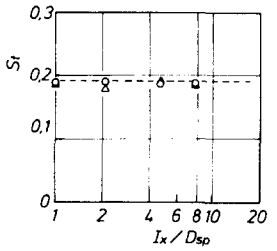

Figure 10. Strouhal number vs longitudinal distance between sphere centers at Re = 430. ○, front sphere; △, rear sphere; ------, single sphere.

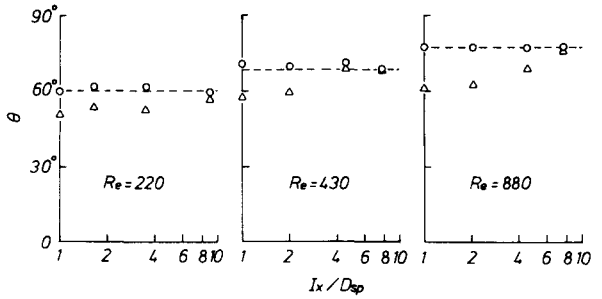

Figure 11. Separation angle vs longitudinal distance between sphere centers. For legends see Fig. 10. (a) $I_Z/D_{sp} = 4.80$; (b) $I_Z/D_{sp} = 2.20$; (c) $I_Z/D_{sp} = 1.48$, (d) $I_Z/D_{sp} = 1$.

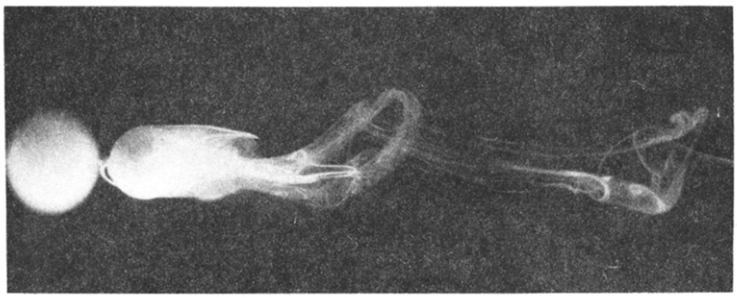

(a)

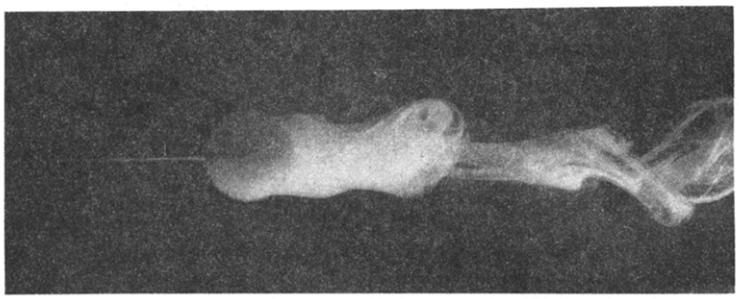

(b)

(c)

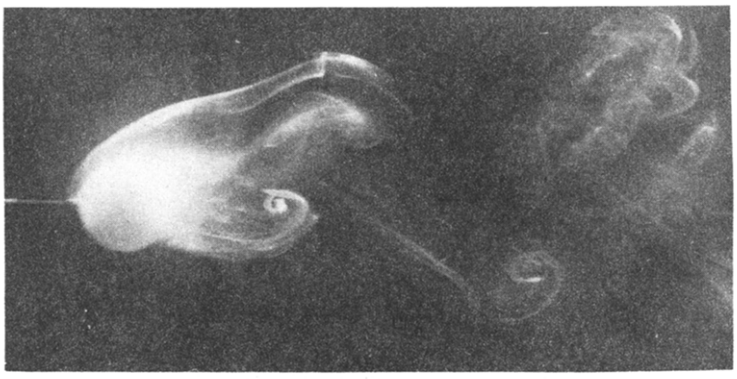

(d)

Figure 12. Side view of vortices in the transverse interaction.

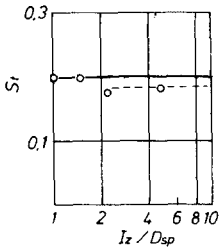

Figure 13. Strouhal number vs transverse distance between sphere centers at Re = 470. ———, single cylinder; ------, single sphere.

vortex. In the case of $I_Z/D_{sp} = 1$, the pattern is almost the same as the Kármán vortex and loses the characters of the vortex of the sphere. Figure 13 shows the relation between the ST number and the transverse distance between the spheres. It is found that St number with small distance is equal to that of the circular cylinder of the same diameter.

4. RESULTS OF THE DRAG COEFFICIENT

The fluid drag on the particle determines particle motion. When solid particles are transported in pipe flow, additional pressure drop is closely related to the drag of each particle. Therefore the drag coefficient is one of the most important factors from a viewpoint of practical use. In fact, most earlier workers of the flow around the sphere have been concerned with the drag coefficient. In this experiment, the sphere of which drag was desired was hung in a stream like a pendulum so that the position of the sphere fluctuated more or less unlike a rigidly supported sphere. Figures 14 and 15 show the records of displacement of the test shpere with and without a dummy sphere in front of the test one. When the dummy sphere was placed ahead of the test sphere, the test sphere fluctuated due to the influence of the dummy sphere. Figure 15 represents the case when the fluctuation was most violent because of a small distance

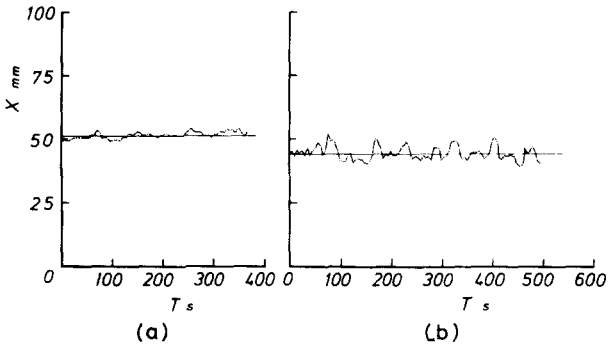

Figure 14. Record of sphere position at Re = 260. (a) single sphere, (b) rear sphere at $I_X/D_{sp} = 2.52$.

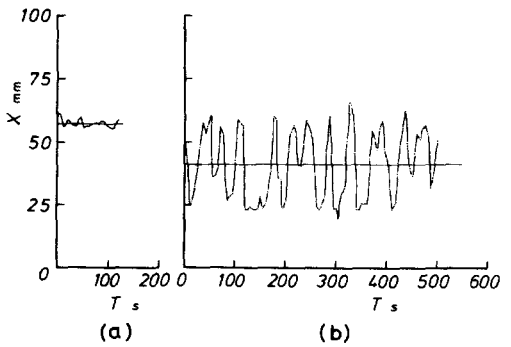

Figure 15. Record of sphere position at Re = 460. (a) single sphere; (b) rear sphere at $I_X/D_{SP} = 1.71$.

between two spheres. However, the frequency of this fluctuation does not correspond to the frequency of the shedding vortex from the dummy (front) sphere but corresponds to the eigen-frequency of the vibration system consisting of a string, a sphere and water, which is much lower than that of the shedding vortices. We took an arithmetrical average of displacement from which the drag coefficient was calculated by using[4]. The present results of C_D without interaction is compared with a standard curve in figure 16 which shows the degree of accuracy of the present measurement. Black circles in the figure represent the results from a group of spheres connected in the transverse direction. That is, the drag force on three spheres was measured with the distance between the spheres sufficiently large, and the drag on one sphere was calculated by dividing the total force by the number of spheres. The drag on the rod was estimated from the relation of the drag on a circular cylinder in a uniform stream. The results obtained in this way show good agreement with the standard curve. This means that the effect of the rod can be estimated in the way mentioned above. One of the reasons of good agreement is that such a group of spheres was hung by two strings which made the position of the group more stable than one string for a single sphere. The ratio of C_D of the rear sphere to C_{D0} of the single sphere is plotted against the non-dimensional distance I_X/D_{sp} in figure 17. The broken line in the figure represents the results by Lee (1979) at high Reynolds numbers. The present results show a large scatter of data so that we do not come to know whether there is a difference according to the Reynolds number. However it can be concluded as a rough estimation that the effect of interaction on the drag coefficient of the rear sphere disappears at the distance I_X/D_{sp} larger than $5 \sim 10$.

Figure 18 shows C_D of the front sphere. The value C_D becomes slightly larger with decreasing distance, which agrees with the result by Lee (1979). Figure 19 shows the results with the transverse interaction. The value shown in the figure are those of the side spheres. It is found that C_D increases with decreasing distance and that the effect of interaction can be neglected at the distance I_Z/D_{sp} larger than $2 \sim 3$.

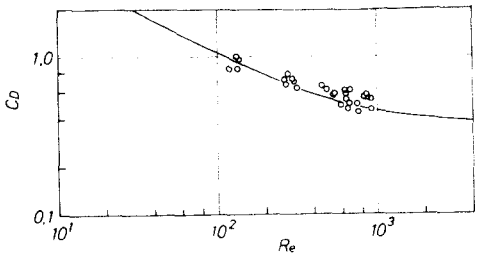

Figure 16. Drag coefficient of single sphere. ———, standard curve; ○, single sphere hung by one string; ●, group of sphere connected by a rod and hung by two strings.

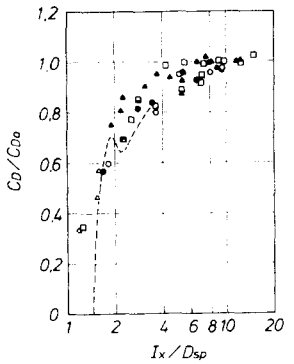

Figure 17. Coefficient ratio of rear to single vs. longitudinal distance between sphere centers. △, Re = 125 ~ 138; ○, Re = 160 ~ 170; □, Re = 312 ~ 330; ●, Re = 556 ~ 580; ▲, Re = 715 ~ 800; -----, Lee (1979).

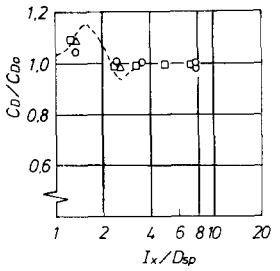

Figure 18. Coefficient ratio of front to single sphere vs longitudinal distance between sphere centers. △, Re = 245; ○, Re = 540; □, Re = 860; -----, Lee (1979).

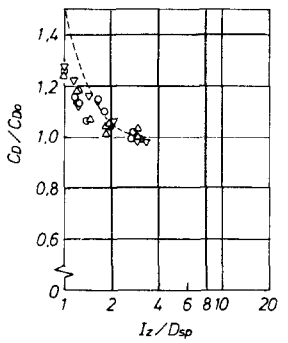

Figure 19. Coefficient ratio of side to single sphere vs longitudinal distance between sphere centers. ○, Re = 360 ~ 370; △, Re = 650 ~ 680; ▽, Re = 810 ~ 870; ------, Lee (1979).

When two circular cylinders are set up normal to the flow in the longitudinal direction, there exists a distance which corresponds to an abrupt change in the values of C_D and St number. There is not such a critical distance in the same condition of spheres. Hence we can say that the effects of interaction are generally monotonous in the case of spheres.

5. CONCLUSIONS

Experiment of fluiddynamic interaction between two spheres was made to obtain basic information about the two-phase flow. Two or three spheres were set up in a water tunnel in the longitudinal or transverse direction with Reynolds numbers less than 10^3. The results are summarized as follows.

(1) The flow behind the sphere was visualized and change in vortex structure due to the interaction was observed. When the two spheres are in the longitudinal direction, only the front vortex changes in structure and the rear vortex is the same as the vortex without interaction. Even at a low Reynolds number where a single sphere does not shed vortices, the front sphere sheds the vortices at a certain distance between the spheres. The stagnation angle on the front sphere is the same as that on the single sphere but the angle decreases on the rear sphere, i.e. the separation position moves down-stream. With respect to the Strouhal number or frequency of the shedding vortices, there is no effect of interaction on both front and rear spheres.

When the spheres are closely placed in the transverse direction, Kármán vortex appears.

(2) Drag force on the sphere were measured by a pendulum method which was developed to detect small drag. The drag of the rear sphere is most largely affected by the interaction, decreasing with decreasing distance between the spheres, but the effect of interaction disappears at a distance larger than $I_X/D_{SP} = 5 \sim 10$, when I_X is the longitudinal distance between the sphere centers and D_{sp} is the diameter of the sphere. As the spheres approach with each other in the transverse direction, the drag increases, but the effect disappears at a distance larger than $I_Z/D_{sp} = 2 \sim 3$, where I_Z is transverse distance between the sphere centers. Differences due to the Reynolds number could not be clarified for lack of accuracy.

Acknowledgement—This work was partially supported by the Grant-in-Aid for Scientific Research from the Ministry of Education in Japan.

REFERENCES

ACHENBACH, E. 1974 Vortex shedding from spheres. *J. Fluid Mech.* **88**, 209–221.

BAGNOLD, R. A. 1974 Fluid forces on a body in shear flow. *Proc. Roy. Soc. Lond.* **A340**, 147–171.

BEARMAN, P. W. & WADCOCK, A. J. 1973 The interaction between a pair of circular cylinder normal to a stream. *J. Fluid Mech.* **61**, 499–511.

ISHIGAI, S., NISHIKAWA, E., NISHIMURA, D. & CHO, K. 1971 Experimental study of structure of gas flow in tube banks with tube axis normal to flow (Part 1, Kármán vortex flow from two tubes at various spacings). *Trans. JSME.* 37–304, 2319–2326 (in Japanese).

KARANFILIAN, S. K. & KOTAS, T. J. 1978 Drag on a sphere in unsteady motion in a liquid at rest. *J. Fluid Mech.* **87**, 85–96.

KNODEL, A. 1926 Über die Gasströmung in Röhren und den Luftwiderstand von Kugeln. *Annalen der Physik* 14–80, 533–587.

LEE, K. C. 1979 Aerodynamic interaction between two spheres at Reynolds numbers around 10^4. *Aero. Quart.* **30**, 371–385.

MAGARVEY, R. H. & BISHOP, R. L. 1961 Wakes in liquid–liquid systems. *Phys. Fluids* **4–7**, 800–805.

MAGARVEY, R. H. & MACLATCHY, C. S. 1965 Vortices in sphere wakes. *Can. J. Phys.* **43**, 1649–1656.

MARCHILDON, E. K. & GAUVIN, W. H. 1979 Effects of acceleration, deceleration and particle shape on single-particle drag coefficients in still air. *AIChE J.* **25**, 938–948.

MÖLLER, W. 1938 Experimentelle Untersuchung zur Hydromechanik der Kugel. *Phys. Z.* **39**, 57–80.

OKAJIMA, A. 1978 Flow around two tandem cylinders at high Reynolds numbers. *Trans. JSME.* 47–384, 2663–2671 (in Japanese).

PERRY, A. E. & LIM, T. T. 1978 Coherent structure in coflowing jets and wakes. *J. Fluid Mech.* **88**, 451–463.

TANEDA, S. 1956 Experimental investigation of the wakes behind cylinders and plates at low Reynolds numbers. *J. Phys. Soc. Japan* **11**, 302–307.

TANEDA, S. 1956 Experimental investigation of the wake behind a sphere at low Reynolds numbers. *J. Phys. Soc. Japan* **11**, 1104–1108.

TANEDA, S. 1978 Visual observation of the flow past a sphere at Reynolds numbers between 10^4 and 10^6. *J. Fluid Mech.* **85**, 187–192.

TOROBIN, L. B. & GAUVIN, W. H. 1959 Fundamental aspects of solids-gas flow (Part 3, Accelerated motion of a particle in a fluid). *Can. J. Chem. Engng* 129–141.

TOROBIN, LK. B. & GAUVIN, W. H. 1960 Fundamental aspects of solids-gas flow (Part 5, The effects of fluid turbulence on the particle drag coefficient). *Can. J. Chem. Engng* 189–200.